

# A New Magnetic Storm Model

Robert B. Sheldon<sup>1</sup> and Harlan E. Spence

*Boston University Center for Space Physics, Boston, Massachusetts*

Recent observations from the new perspective of the POLAR orbit have elucidated the crucial role that parallel electric fields and the ionosphere play in the development of a magnetic storm. During the main phase, we observed field-aligned beams of ionospheric ions that appear to be caused by deeply convecting plasmashet ions. These ionospheric beams are a substantial fraction of the ring current density, suggesting a novel mechanism for ring current and Dst growth during the main phase of a magnetic storm. From these observations, we construct a new magnetic storm model that has implications for all aspects of a storm sequence, including ground, ionospheric and magnetospheric observations.

## 1. INTRODUCTION

The elements of this new magnetic storm model have all been presented before, but they have lacked a coherent, causal chain, that could connect them with the “standard ring current storm model” [e.g., *Smith and Hoffman(1974)*; *Gonzalez et al.(1994)*]. This “standard model” supposes that the generation of an enhanced cross-tail convection electric field during a storm convects in the near Earth plasmashet into the ring current region on open drift paths. The abrupt cessation of this electric field strands the plasma in the ring current (RC), on now closed drift paths.

As attractive as this model is, it has a number of drawbacks. First, the injection of RC plasma is initially on open drift paths, so that the current contents of the RC are emptied as the new plasma arrives. This makes multiple injections difficult to accomplish, since as much RC is being lost as injected. Thus the only way a Dst effect could be accomplished, would be if the plasmashet density were higher than RC density. In general, the RC is in diffusive equilibrium with the plasmashet [ *Sheldon(1994a)*], so that a “superdense” plasmashet increase is required to produce a large Dst storm. This prerequisite (which is only weakly supported by the data) adds complication to the simple model above. Yet even with this included, models of the storm-time RC generation, [e.g., *Fok et al.(1995)*; *Jordanova(1998)*] find that there remains a factor 2 discrepancy between simulated and actual Dst. Or if the boundary condition is adjusted to produce enough Dst, the RC during storm recovery is too large.

*Chen et al.*(1993) recognized that this abrupt cessation of electric field on a timescale shorter than the drift time would violate the 3rd invariant, leading to radial diffusion. They then explored multiple electric field pulses, showing that rapid diffusion could also generate the RC from a plasmashet source. This had the advantage that multiple injections were cumulative, but the same disadvantage that the final RC energy content remained dependent on plasmashet densities.

A second objection to the standard model came from composition analysis of the storm-time RC. *Hamilton et al.*(1988) measured the enhanced ionospheric oxygen content of great storms, far above the quiescent  $H^+/O^+$  RC ratio. This ratio was shown to be proportional to Dst [ *Grande et al.*(1997)], which again, suggests that the plasmashet must be “prepared” for a great storm. Yet despite the work of *Daglis and Axford*(1996), no such mechanism operating on storm timescales was found.

Our model takes as its input the cross-tail potential at the inner edge of the plasmashet and the plasmashet density at this location, to predict the abrupt Dst change as well as the subsequent recovery and compositional changes in a complete storm sequence. With a suitable inner tail model, we should be able to use only the solar wind density and electric field,  $E_y = B_z \times V_x$ , to make these predictions.

## 2. DATA ANALYSIS

The POLAR spacecraft is in a polar,  $9 \times 2$  Re orbit that on April 15, 1996, was in the noon-midnight meridian with perigee over the south pole. Thus it made two diagonal passes through the midnight and noon radiation belts. A typical pass shows an energetic particle population whose average energy is proportional to the  $|B|$ . This is the normal distribution for ions diffusing in L-shell from a source region in the plasmashet. On this day the Comprehensive Energetic Particle and Pitch Angle Distribution (CEPPAD) [ *Blake et al.*(1995)] experiment detected two nearly monoenergetic bands superposed on the night side ring current (plate 1): a population of trapped ions at  $\sim 90$  keV, and a beam of field-aligned ions at  $\sim 40$  keV.

A nearly monoenergetic trapped population is possible when a strong cross-tail electric field drives ions against the  $\nabla B$  and corotation  $E \times B$  drifts deep into the magnetosphere [ *Smith and Hoffman*(1974); *Sheldon*(1994b)]. Such a “nose” event must be nearly  $90^\circ$  trapped particles because of the large increase in  $|B|$  while convecting from the plasmashet, which is the

characteristic of the upper energy band in our data. Since nose events are highly correlated with storms, and storms are defined by Dst, but Dst is generally not immediately available, we turn to the preliminary Dst provided by the Kyoto University web site. After subtracting the ionospheric Sq contribution using the “quietest day of the month” (April 7/8) method, we find a moderate storm of at least -63 nT on the first hour of April 15. Additional support for the nose event identification came from the extensive GGS database.

Examination of WIND data [ *Ogilvie et al.(1995)*] for April 14 showed that there were several  $Bz < 0$  periods lasting for 1 hour or less. Corresponding CU and CL derived from the CANOPUS array [ *Rostoker et al.(1995)*] show that these periods led to substorms with riometer absorption signatures at auroral latitudes. However the storm trigger appears to be the strong southward turning of  $Bz < -10$  occurring at 2000 UT, accompanied by a jump in the solar wind speed from 450 km/s to 600 km/s, which produced an even larger  $Bz$  in the compressed magnetic field of the magnetosheath. This period of strong southward  $Bz$  lasted more than 3 hours, effectively saturating the ability of the tail to shield out the polar cap potential. The IZMIRAN model [ *Papitashvili et al.(1994)*] predicted in excess of 150 kV across the polar cap for these solar wind conditions.

The CANOPUS array detected a magnetic bay, a nearly equal response of AU and AL, suggesting that the current systems had moved equatorward, overhead of the magnetometers. Indeed, the Halley Bay magnetometer at  $L \sim 4$  [ *Dudney et al.(1995)*] showed a large H deflection with almost no Z deflection, indicative of strong overhead currents. The ionosphere responded strongly at this time (private communication, J. Aarons, 1996) as ionospheric scintillations were enhanced.

While CANOPUS riometers at  $L > 6$  recorded very little activity, the riometer at  $L = 4.4$  as well as the Halley Bay riometer at  $L \sim 4$ , (private communication A. Rodger, 1996) showed an extremely intense and narrow absorption feature at this time, indicating that precipitation had penetrated to low latitudes, deep in the magnetosphere and down to E-layer ionospheric depths. From these observations, as well as complementary ground observations, we surmise that after several intense substorms had pumped up the plasmasheet, a strong convection field injected the plasma to at least  $L = 4.4$ , which POLAR/ CEPPAD observed as a 90-100 keV band.

The band of 40 keV field-aligned ions, however, are harder to explain. They have the wrong pitchangles to

have convected from the plasmashet, because the adiabatic decompression involved in backtracing them to their origin would place them in the plasmashet loss cone. Nor would ions of this energy have had access to the plasmashet simultaneously with higher energy ions, since the magnetosphere is a “notch filter” for only one energy. This implies that these ions are trapped on closed drift orbits. But if they undergo the same processes as the adiabatically energized ring current, which can be seen simultaneously with the banded distribution, they would not be monoenergetic, nor would they track the energy of the nose ions so precisely. That is, if they had resided for any length of time in the magnetosphere, the same convection that brought in the plasmashet ions would disperse these ions as well. Nor do these ions show the energy dispersion associated with substorm injections. Thus we conclude that these field-aligned ions are *in situ* accelerated during the time of the measurement.

“Zipper” events, [ *Fennell et al.* (1981); *Kaye et al.* (1981)], have the same bimodal pitch-angle distributions, though at somewhat lower energy. They found that the “zippers” were rich in  $O^+$ , and concluded that they were observing beams coming from the ionosphere. Since beams are seen at auroral latitudes, they concluded that they were on flux tubes connected to auroral arcs. The composition experiment on POLAR, CAMMICE, was turned off during this period, so we cannot determine the  $E > 30\text{keV } O^+$  content for April 15, however when it was switched back on, around April 19, it found an anomalously large amount of  $O^+$  in the ring current (RC) in two energy bands centered at 40 and 100 keV. Because of the short lifetime of  $O^+$  against charge exchange, such a measurement is consistent with a storm injection occurring only a few days previously, since between storms, CAMMICE detects no  $O^+$  enhancements. A similar storm on March 21, 1996 showed that the IPS zippers are simultaneous with the double peaked  $O^+$  spectrum observed by CAMMICE. And POLAR/ TIMAS [ *Shelley et al.*(1995)] (private communication W.K. Peterson, 1996) did detect  $E < 20\text{keV } O^+$  beams for this day. So we conclude that on April 15 we are observing  $O^+$  ions accelerated to  $\sim 30\text{--}40\text{ keV}$  by strong parallel electric fields in the ionosphere. Since these ions track  $\sim 50\text{ keV}$  below the nose ions, it appears there must be a causal connection.

*Whipple*(1977) argues that one can produce a field-aligned electric field if the electron and ion pitch angle distributions (PADs) are not identical. In our case, a hot monoenergetic nose ion superposed on a cold plasmashet electron population will produce a parallel

electric field of several  $kT_e$  pointing away from the equator. That is, since a mirroring ion spends most of its time away from the equator, the electrons at the equator will experience a force pulling them toward higher latitudes. If the energetic ion density (or current density in a dynamic system) is greater than the plasmaspheric cold electron density, a second ion-dominated solution to the Whipple equations is possible that produces an ion space-charge potential at approximately the ion beam parallel energy. (Since the Whipple equations are derived for a neutral plasma, we must re-derive these results using Poisson's equation for a non-neutral plasma. Intriguing evidence that such space charge is both possible and probable come from laboratory experiments on magnetized, trapped electron clouds *Hansen and Fajans(1995)*) This space charge potential would expel magnetospheric electrons to the equator and could only be neutralized somewhere earthward on the flux tube where the cold electron density would again exceed the hot ions. At this point, the potential would drop from kV to a few  $kT_e$ , forming a double layer. Naturally this space charge should be shielded by neighboring flux tubes, generating a locally perpendicular electric field that may be manifest in the ionosphere by a "polarization jet" or a subauroral ion drift (SAID).

By measuring the energy of these beams as the spacecraft crosses through this region, we can map out some features of this potential structure. We have fit the spectra with a sum of three peaks: a Chapman layer function appropriate for the ionospheric beam, a Gaussian for the nose ions, and a log-space Gaussian for the ring current ions, achieving remarkably good 9 parameter fits to 16 energy points. We note that an asymmetric Chapman layer function,  $y = \exp(1 + x - \exp(x))$ , is what one expects if the extraction potential is extended over some distance.

Figure 1 demonstrates how the three populations, beam, nose and RC, evolve during this orbit. The RC is adiabatically energized so that as the model equatorial magnetic field increases the energy increases, as noted by the squares and dashed line. A latitude effect in RC is apparent due to the more rapid loss of low energy ions at higher latitudes. This energization is not seen by the nose ions because they are not an equilibrium trapped population, rather we are seeing the nose ions that have access to this location, so that stronger B-field ions also began with smaller magnetic moment. A more detailed analysis of the pitch angles is needed to clarify the coupled energy-L dependence of these ions.

If the first solution of *Whipple* holds, then both the

nose and the beam energies should move in concert as we move along the field line, and we should observe a constant difference between these two energies (circles). We find instead that the ratio ( $X$ ) is more constant, that the beam ion energy tracks the nose ion energy with a nearly constant ratio of  $1/2$ . This suggests that the beam energy is determined not by the electron thermal temperatures or anisotropies, but by the energy of the nose ions themselves, consistent with the second, ion-dominated solution to the *Whipple* equilibrium.

Such a parallel electric field should also accelerate magnetospheric electrons to 30 keV into the ionosphere, producing a riometer absorption event. Since the electric field is colocated with the nose plasma, the absorption must be a narrow strip in latitude but distributed in longitude, as seen in the CANOPUS data. This extended signature is reminiscent of SAIDs which have been previously identified with substorm injections. Our mechanism would identify a large SAID with a storm injection, and which may also account for the E-layer keV electron signature seen in subauroral riometer data.

We carefully distinguish between substorm and storm injections because the characteristic signatures of each are different. A substorm involves a reconfiguration of the magnetic field which produces a  $dB/dt$  electric field in the region between 6-10 Re near midnight. This produces two types of signatures in the POLAR data. The inductive electric field may *in situ* accelerate the entire plasma population to  $\sim 30$  keV, which is observed in our instrument as an isotropic, dispersionless  $< 50$  keV enhancement over a restricted MLT and L-shell range. Or it may bring in plasmashet material with a distinctive, highly energy dispersed signature. A storm injection, on the other hand, is observed as a nose event, a monoenergetic band of ions penetrating to subauroral L-shells and existing over a broad range of MLT determined by the duration of the cross-tail field. Energization of low energy plasma is not seen, but adiabatic energization of the nose ions occurs as the ions convect toward stronger B. From an ionospheric viewpoint, substorms are in the auroral zone, whereas storms penetrate down to subauroral latitudes albeit in a restricted latitude band. Thus we argue that these beams cannot be substorm generated.

### 3. DISCUSSION

If our mechanism generates field aligned electric fields and oxygen rich beams for every storm injection, then we have elucidated a new model for magnetic storms.

Since it is generally thought that magnetic storms are characterized by intense convection fields that bring plasmasheet plasma deep into the RC, then all storms should create parallel fields and extract oxygen from the ionosphere as well. Thus large storms should extract more oxygen than small storms, with a larger Dst effect. Similarly, Dst should change on minute bounce timescales, rather than the 10's of minutes convection timescales.

Several recent observations lend support for this theory. Analysis of the CRRES data set shows that there is a positive correlation between the magnitude of Dst and the  $O^+$  content of the RC [ *Grande et al.(1997)*]. A Dst prediction filter [ *Gleisner et al.(1996)*] found that a neural network with one hidden layer, representing an unknown quadratic dependence on solar wind  $V_x, B_z$ , and density, could explain up to 84% of the variance in Dst, an improvement over the linear filter's 70%. If significant  $O^+$  is extracted during the main phase as we predict, one would expect such a non-linear dependence of Dst with  $E_y$ . In addition, Kyoto 1-minute Dst show excursions much too rapid for convective timescales.

A study of storm-time PC1 pulsations by *Mursula* (COSPAR 1996 paper to be published in *Adv. Sp. Res.*) showed that the PC1 waves associated with ion-cyclotron waves during the most intense part of the main phase of a storm occurred primarily at dusk and the PC1 frequency dropped down to below the oxygen gyrofrequency. These observations are suggestive of an oxygen rich plasma occurring at dusk, the location of the deepest penetration of the nose ions and also in agreement with our theory.

This extraction of ions and precipitation of electrons near midnight will generate an outward flowing current which then drifts westward with the bulk of the RC. We expect that the disappearance of the parallel field, occurring near the dusk terminator, will result in a downward current thus completing the loop of the partial ring current as measured by *Suzuki et al.(1985)* using Magsat data. They concluded that 1/3-1/4 of RC amperage was observed in the partial RC. If we assume that half of the partial RC is carried by upward flowing ions, then we estimate that 1/6 - 1/8 of the total RC is composed of ions of ionospheric origin.

Finally, if electrons are being precipitated into the ionosphere, one would expect the generation of X-rays. POLAR/PIXIE has observed an intense emission in a single spot near the dusk terminator that occurs midway through main phase of almost every major Dst storm [ *Imhof et al.(1998)*]. This global observation is again consistent in location and timing with our accel-

eration mechanism.

Thus we find that the mechanism described in the abstract not only provides a causal chain for the entire storm sequence, but has great predictive power in explaining many other observations not previously linked to storms.

#### 4. CONCLUSIONS

We have attempted to construct a new model of magnetic storms that incorporates field-aligned electric fields as an intrinsic part of the storm development. A storm proceeds then with the following steps: 0) A critical density plasmashet may be required for a significant magnetic storm, in which case precursor substorm activity or a solar wind density enhancement would be a prerequisite. 1) Large solar wind  $E_y$  produces a large polar cap electric field, which if persistent for an extended period ( $>3$ hr) exceeds the ability of the tail to shield out the electric field. 2) This produces a strong cross-tail convection electric field that transports plasmashet ions deep into the magnetosphere. 3) The opposing  $\nabla B$  and  $E \times B$  drifts act as a selective filter permitting a single energy the deepest penetration, a monoenergetic “nose” event. 4) This spatially narrow band of hot ions, compressed as it convects towards stronger  $B$  reaches its highest density near the dusk terminator where it can outnumber the local cold electron density at the equator and thus generate a field-aligned space-charge potential that attempts to confine the hot ions to the equator, a parallel electric field. 5) At some point down the field line earthward of the equator, the growing cold electron density exceeds the hot ions and the potential is neutralized to approximately the electron thermal temperature, forming a double layer that very quickly extracts ionospheric ions, including  $H^+$  and  $O^+$ . 6) Ion cyclotron waves, generated by this unstable particle population, then perpendicularly heat these ion beams and scatter them out of the loss cone so that they become a permanent part of the ring current. 7) This entire structure is a “convection instability”, a dynamic balance between the current of corotating cold electrons and convecting hot ions, which would rapidly decay if it were not for the continuous power input of the convection electric field. When the field switches off, the convection power source is removed, the parallel electric fields vanish, and the hot ions are trapped in the ring current and subsequently decay through charge exchange.

*Acknowledgments.* This study was supported by NASA contract NAS5-30368 and NSF grant ATM-9458424. The authors gratefully acknowledge K. Ogilvie, E. Shelley, J. Dudeney, G. Rostoker, B. Blake and T. Fritz for the use of their data.

## REFERENCES

- Blake, J. B. et al. CEPPAD: Comprehensive energetic particle and pitch angle distribution experiment on POLAR. In C. T. Russell, editor, *The Global Geospace Mission*, pages 531–562. Kluwer Academic Publishers, 1995.
- Chen, M. W., M. Schulz, L. R. Lyons, and D. J. Gorney. Stormtime transport of ring current and radiation-belt ions. *J. Geophys. Res.*, *98*, 3835–3849, 1993.
- Daglis, I. A. and W. I. Axford. Fast ionospheric response to enhanced activity in geospace: Ion feeding of the inner magnetotail. *J. Geophys. Res.*, *101*, 5047–5065, 1996.
- Dudeney, J. R. et al. Satellite experiments simultaneous with antarctic measurements (SESAME). In C. T. Russell, editor, *The Global Geospace Mission*, pages 705–742. Kluwer Academic Publishers, 1995.
- Fennell, J. F., D. R. Croley, Jr., and S. M. Kaye. Low-energy ion pitch angle distributions in the outer magnetosphere: Ion zipper distributions. *J. Geophys. Res.*, *86*, 3375, 1981.
- Fok, M.-C., T. E. Moore, J. U. Kozyra, G. C. Ho, and D. C. Hamilton. Three-dimensional ring current decay model. *J. Geophys. Res.*, *100*, 9619–9632, 1995.
- Gleisner, H., H. Lundstedt, and P. Wintoft. Predicting geomagnetic storms from solar-wind data using time-delay neural networks. *Ann. Geophys.*, *14*, 679–686, 1996.
- Gonzalez, W. D., J. A. Joselyn, Y. Kamide, H. W. Kroehl, G. Rostoker, B. T. Tsurutani, and V. M. Vasyliunas. What is a geomagnetic storm? *J. Geophys. Res.*, *99*, 5771–5792, 1994.
- Grande, M., C. H. Perry, A. Hall, J. Fennell, and B. Wilken. Survey of ring current composition during magnetic storms. *Adv. Space Res.*, *20*, 321–326, 1997.
- Hamilton, D. C. et al. Ring current development during the great geomagnetic storm of february 86. *J. Geophys. Res.*, *93*, 14,343–14,355, 1988.
- Hansen, C. and J. Fajans. Debye shielding and the dynamic response of a magnetized, collisionless plasma. In *Non-Neutral Plasma Physics II*, volume AIP Conference Proceedings 331, pages 87–91, New York, 1995.
- Imhof, W. L., D. L. Chenette, D. W. Datlowe, J. Mobilia, M. Walt, and R. R. Anderson. The correlation of AKR waves with precipitating electrons as determined by plasma wave and x-ray image data from the POLAR spacecraft. *Geophys. Res. Lett.*, *25*, 289–292, 1998.
- Jordanova, V. K. October 1995 magnetic cloud and accompanying storm activity: Ring current evolution. *J. Geophys. Res.*, *103*, 79, 1998.
- Kaye, S. M. et al. Ion composition of zipper events. *J. Geophys. Res.*, *86*, 3383–3388, 1981.
- Ogilvie, K. W. et al. Swe, a comprehensive plasma instrument for the wind spacecraft. In C. T. Russell, editor, *The Global Geospace Mission*, pages 55–77. Kluwer Academic Publishers, 1995.
- Papitashvili, V. O. et al. Electric potential patterns in the

northern and southern polar regions parameterized by interplanetary magnetic field. *J. Geophys. Res.*, 99, 13,251, 1994.

Rostoker, G. et al. Canopus - a ground-based instrument array for remote sensing the high latitude ionosphere during the istp/ggs program. In C. T. Russell, editor, *The Global Geospace Mission*, pages 743–760. Kluwer Academic Publishers, 1995.

Sheldon, R. B. Ion transport and loss in the earth’s quiet ring current 2. diffusion and magnetosphere-ionosphere coupling. *J. Geophys. Res.*, 99, 5705–5720, 1994a.

Sheldon, R. B. Plasmasheet convection into the inner magnetosphere during quiet conditions. In D. N. Baker, editor, *Solar Terrestrial Energy Program: COSPAR Colloquia Series*, volume 5, pages 313–318, New York, 1994b. Pergamom Press.

Shelley, E. G. et al. The toroidal imaging mass-angle spectrograph (TIMAS) for the POLAR mission. In C. T. Russell, editor, *The Global Geospace Mission*, pages 497–530. Kluwer Academic Publishers, 1995.

Smith, P. and R. Hoffman. Direct observations in the dusk hours of the characteristics of the storm time ring current particles during the beginning of magnetic storms. *J. Geophys. Res.*, 79, 966, 1974.

Suzuki, A., M. Yanagisawa, and N. Fukushima. Anti-sunward space current below the magsat level during magnetic storms, and its possible connection with partial ring current in the magnetosphere. *J. Geophys. Res.*, 90(B3), 2465–2471, 1985.

Whipple, Jr, E. C. The signature of parallel electric fields in a collisionless plasma. *J. Geophys. Res.*, 82, 1525, 1977.

---

Robert B. Sheldon, Boston University Center for Space Physics, rsheldon@bu.edu

---

<sup>1</sup>now at The University of Alabama in Huntsville, Huntsville, Alabama

A NEW MAGNETIC STORM MODEL	SHELDON AND SPENCE
A NEW MAGNETIC STORM MODEL	SHELDON AND SPENCE
A NEW MAGNETIC STORM MODEL	SHELDON AND SPENCE
A NEW MAGNETIC STORM MODEL	SHELDON AND SPENCE
A NEW MAGNETIC STORM MODEL	SHELDON AND SPENCE
A NEW MAGNETIC STORM MODEL	SHELDON AND SPENCE
A NEW MAGNETIC STORM MODEL	SHELDON AND SPENCE
A NEW MAGNETIC STORM MODEL	SHELDON AND SPENCE
A NEW MAGNETIC STORM MODEL	SHELDON AND SPENCE

**Figure 1.** Peak fits to 96s averaged spectra of the 90° head. Ring current ( $\square$ ), nose ion ( $*$ ), beam ion ( $\triangle$ ) energies, difference ( $\circ$ ) and 10 $\times$  the ratio ( $\times$ ) of nose:beam are plotted. “Error” bars are FWHM from fits, since fitting errors are negligible. Overplotted with different scales are: one half the model equatorial B-field intensity (dashed); and on linear scale the magnetic latitude from -40 to 40 degrees (dotted), with the equator marked with a vertical dotted line.

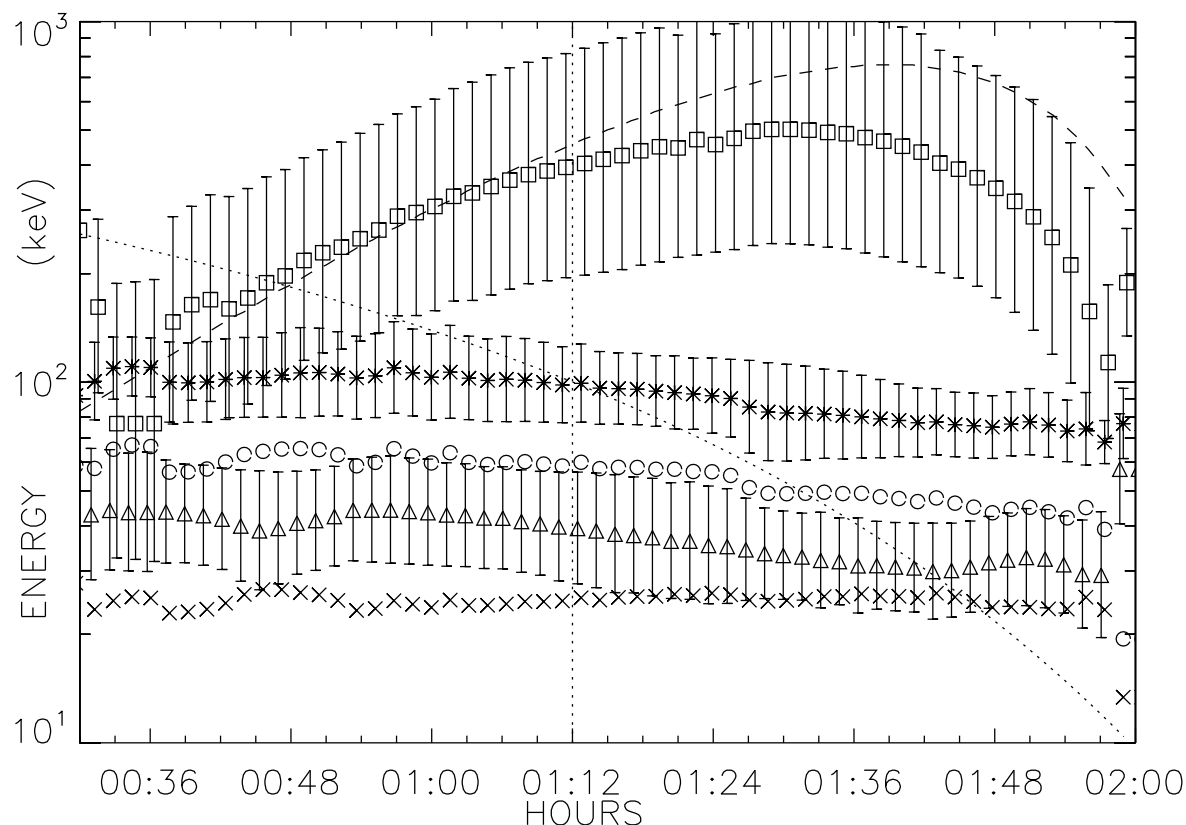


**Figure 1.** Peak fits to 96s averaged spectra of the 90° head. Ring current ( $\square$ ), nose ion ( $*$ ), beam ion ( $\triangle$ ) energies, difference ( $\circ$ ) and 10 $\times$  the ratio ( $\times$ ) of nose:beam are plotted. “Error” bars are FWHM from fits, since fitting errors are negligible. Overplotted with different scales are: one half the model equatorial B-field intensity (dashed); and on linear scale the magnetic latitude from -40 to 40 degrees (dotted), with the equator marked with a vertical dotted line.

**Plate 1.** POLAR/ CEPPAD/ IPS data on April 15, 1996, displaying roll modulation of the counts in the 90° head in the energy bands from 24–138 keV. Dotted white and blue lines are 90° and 60° pitchangles.

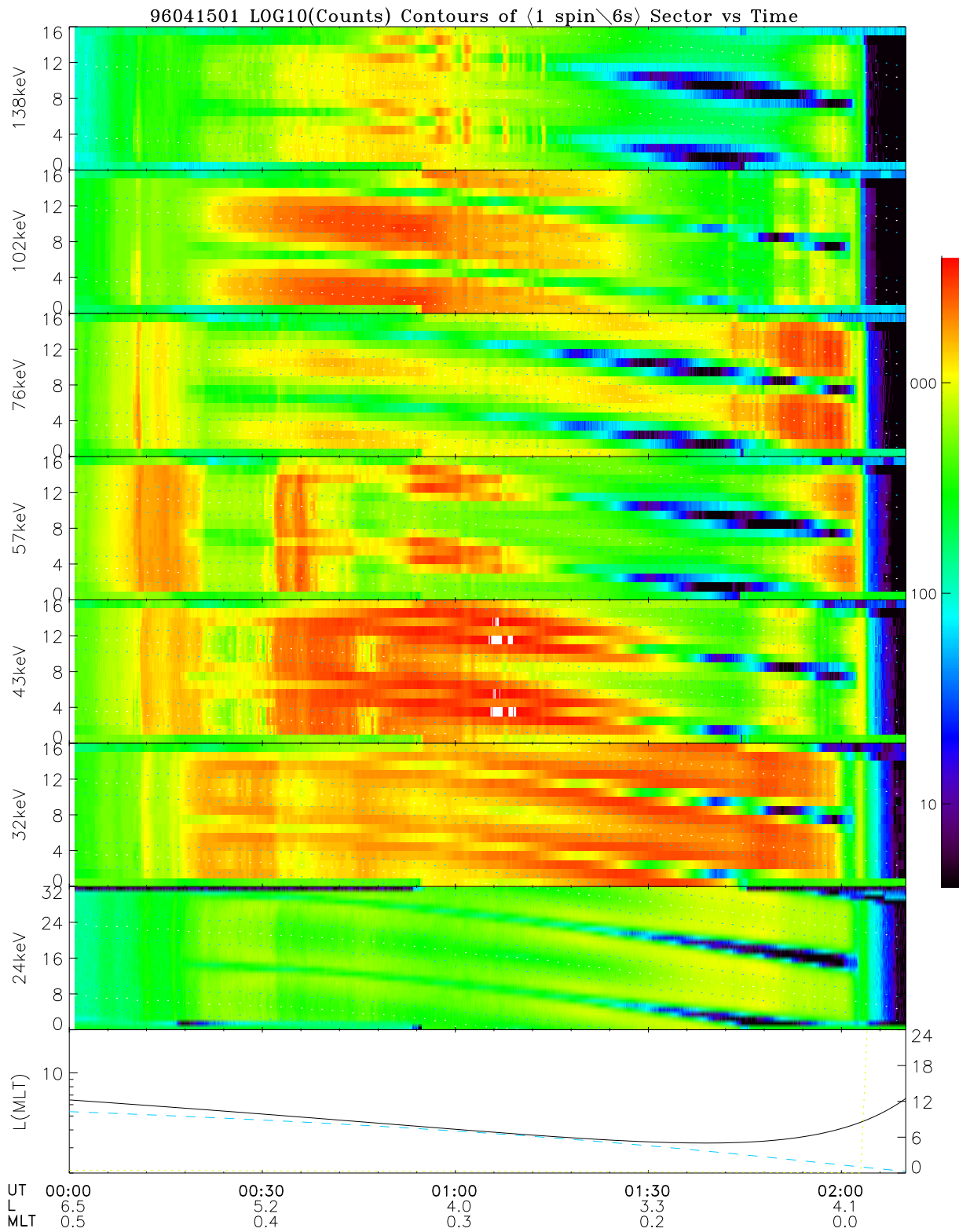


**Plate 2.** POLAR/ CEPPAD/ IPS data on April 15, 1996, displaying roll modulation of the counts in the 90° head in the energy bands from 24–138 keV. Dotted white and blue lines are 90° and 60° pitchangles.